*Progress In Electromagnetics Research B, Vol. 6, 81–92, 2008*

# FSS COMPRISED OF ONE- AND TWO-TURN SQUARE SPIRAL SHAPED CONDUCTORS ON DIELECTRIC SLAB

**K. Delihacioglu**

Department of Physics
Faculty of Art and Science
Kilis 7 Aralık University
79100 Kilis, Turkey

**S. Uckun and T. Ege**

Electrical and Electronics Engineering Department
University of Gaziantep
Gaziantep 27310, Turkey

**Abstract**—The scattering of electromagnetic waves from a Frequency Selective Surfaces (FSSs) composed of a new one- and two-turn square spiral shaped periodic structures are investigated by using modal expansion method for a linearly polarized transverse electric (TE) and transverse magnetic (TM) incident waves. The Moment Method (MM) of Galerkin type is employed by expressing the current induced on the metallic surfaces in terms of Piecewise Sinusoidal (PWS) basis functions to determine the FSS structure reflection and transmission coefficients.

## 1. INTRODUCTION

Frequency selective surfaces (FSSs) have transmission and reflection properties which vary with frequency. FSSs comprised of periodically arranged metallic elements or aperture elements within a metallic screen exhibit total reflection or transmission. Some applications of FSSs are band stop filters, band pass filters, microwave multiband antennas, hybrid radomes, dichroic subreflectors, etc. [1, 2]. The numerical analysis algorithm for the square spiral antennas is developed by Nakano expanding the current distribution in Piecewise Sinusoidal (PWS) basis functions [3]. Scattering from the perfectly

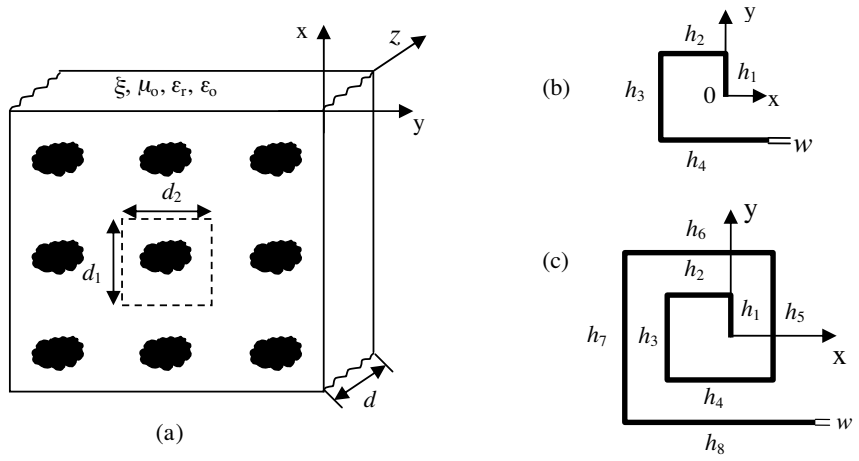


**Figure 1.** (a) FSS composed of infinite doubly periodic conductors printed on a dielectric slab. (b) One-turn square spiral FSS element. (c) Two-turn square spiral FSS element.

conducting arrays of different FSS structures have been analyzed and reported by many authors. The reflection and transmission coefficients of two new FSSs which are made up of one- [4] and two-turn square spiral [5] shaped conducting strips, as shown in Figures 1(b) and 1(c) are investigated in this study. The FSSs of periodic square spiral elements can be designed to reflect frequencies in the X- (8–12.5 GHz) and Ku-bands (12.5–18 GHz), while it is completely transparent in S-band (1–5 GHz) frequency region.

## 2. FORMULATION OF THE FSS SCATTERING PROBLEM

The geometry of an infinite doubly periodic array of two dimensional scatterers is shown in Figure 1. The basic structure is constructed with the periodic arrangement of thin one- and two-turn square spiral shaped conducting strips printed on a dielectric substrate. The lengths ($h_n$) and the width ($w$) of the FSS structures are shown in Figures 1(b) and 1(c). The periodicities ($d_1$ and $d_2$), substrate thickness ($d$) and dielectric constant ($\varepsilon_r$) are shown in Figure 1(a). In this study, the modal expansion of the fields is used in conjunction with the Moment Method (MM) [6] of Galerkin type to determine the induced current coefficients, reflection and transmission characteristics for both types of FSS structures. We introduce scalar and vector field expansion of

Floquet [7] modes of an arbitrary periodic array. The FSS array is illuminated by a monochromatic plane wave of arbitrary polarization (either TE or TM incident) from the free space region. The amplitude of the incident electric field is set to unity (1 V/m). The incident, reflected and transmitted fields can be found in [8]. The incident electric field will induce currents on FSS elements which in turn will be scattered in the forward and backward directions.

The total transverse incident electric and magnetic fields in the region $z \leq 0$ in the absence of the scatterers is given by [8],

$$\boldsymbol{E}_t^{\text{inc}} = \sum_{r=1}^{2} [e^{-j\gamma_{00}^o z} + R_{r00}^{\text{slab}} e^{j\gamma_{00}^o z}] b_r^{\text{inc}} e^{-j\boldsymbol{k}_{00}\cdot\boldsymbol{\rho}} \boldsymbol{\kappa}_{r00} \tag{1}$$

$$\boldsymbol{H}_t^{\text{inc}} = \sum_{r=1}^{2} Y_{r00}^o [e^{-j\gamma_{00}^o z} - R_{r00}^{\text{slab}} e^{j\gamma_{00}^o z}] b_r^{\text{inc}} e^{-j\boldsymbol{k}_{00}\cdot\boldsymbol{\rho}} \boldsymbol{a}_z \times \boldsymbol{\kappa}_{r00} \tag{2}$$

where the subscript $t$ indicates the transverse field component and $b_r^{\text{inc}}$ is the amplitude of incident field. The modal admittances of the free space in the region $z \leq 0$ and $z \geq d$ are given by,

$$Y_{1pq}^o = \frac{k_o Y_o}{\gamma_{pq}^o}, \quad Y_{2pq}^o = \frac{\gamma_{pq}^o Y_o}{k_o}, \quad Y_o = \sqrt{\varepsilon_o/\mu_o}, \quad k_o = \omega\sqrt{\varepsilon_o \mu_o},$$

$$\gamma_{pq}^o = \begin{cases} \sqrt{k_o^2 - |\boldsymbol{k}_{pq}|^2} & k_o \geq |\boldsymbol{k}_{pq}| \\ -j\sqrt{|\boldsymbol{k}_{pq}|^2 - k_o^2} & k_o \leq |\boldsymbol{k}_{pq}| \end{cases}$$

$$\varepsilon_o = \frac{10^{-9}}{36\pi}\,\text{F/m} \quad \mu_o = 4\pi 10^{-7}\,\text{H/m}$$

where $\varepsilon_o$, $\mu_o$ are the permittivity and permeability of the free space. The reflection coefficient, $R_{rpq}^{\text{slab}}$ at the boundary at $z = 0$, due to the dielectric slab is given by

$$R_{rpq}^{\text{slab}} = \frac{2Y_{rpq}^o - Y_{rpq}^{eq}}{Y_{rpq}^{eq}} \tag{3}$$

where $Y_{rpq}^{eq}$ is the equivalent modal admittance given as

$$Y_{rpq}^{eq} = Y_{rpq}^o + Y_{rpq}\left(\frac{1 - R_{rpq}}{1 + R_{rpq}}\right), \quad Y_{1pq} = \frac{kY}{\gamma_{pq}},$$

$$Y_{2pq} = \frac{\gamma_{pq} Y}{k}, \quad Y = \sqrt{\varepsilon/\mu} \quad R_{rpq} = \left[\frac{Y_{rpq} - Y_{rpq}^o}{Y_{rpq} + Y_{rpq}^o}\right] e^{-j2\gamma_{pq} d}$$

Equation (3) is found in a straightforward manner by matching the tangential electric and magnetic fields at $z = 0$ and $z = d$.

The incident wave induces current on the scatterers. Radiation from the current and scattering from the dielectric slab yield the electromagnetic fields. The scattered fields in region $1\,(z \leq 0)$, $2\,(0 < z < d)$ and $3\,(z \geq d)$ are represented by $\{\boldsymbol{E}_1, \boldsymbol{H}_1\}$, $\{\boldsymbol{E}_2, \boldsymbol{H}_2\}$ and $\{\boldsymbol{E}_3, \boldsymbol{H}_3\}$, respectively. For $z \leq 0$, we have

$$\boldsymbol{E}_1 = \sum_{r=1}^{2} \sum_{p=-\infty}^{\infty} \sum_{q=-\infty}^{\infty} a^{-}_{rpq} e^{j\gamma^{o}_{pq} z} \cdot e^{-j\boldsymbol{k}_{pq}\cdot\boldsymbol{\rho}} \boldsymbol{\kappa}_{rpq} \tag{4}$$

$$\boldsymbol{H}_1 = -\sum_{r=1}^{2} \sum_{p=-\infty}^{\infty} \sum_{q=-\infty}^{\infty} Y^{o}_{rpq} a^{-}_{rpq} e^{j\gamma^{o}_{pq} z} \cdot e^{-j\boldsymbol{k}_{pq}\cdot\boldsymbol{\rho}} (\boldsymbol{a}_z \times \boldsymbol{\kappa}_{rpq}) \tag{5}$$

In the region $0 < z \leq d$,

$$\boldsymbol{E}_2 = \sum_{r=1}^{2} \sum_{p=-\infty}^{\infty} \sum_{q=-\infty}^{\infty} [b_{rpq} e^{-j\boldsymbol{\gamma}_{pq} z} + a_{rpq} e^{j\boldsymbol{\gamma}_{pq} z}] \cdot e^{-j\boldsymbol{k}_{pq}\cdot\boldsymbol{\rho}} \boldsymbol{\kappa}_{rpq} \tag{6}$$

$$\boldsymbol{H}_2 = \sum_{r=1}^{2} \sum_{p=-\infty}^{\infty} \sum_{q=-\infty}^{\infty} Y_{rpq} [b_{rpq} e^{-j\boldsymbol{\gamma}_{pq} z} - a_{rpq} e^{j\boldsymbol{\gamma}_{pq} z}] \cdot e^{-j\boldsymbol{k}_{pq}\cdot\boldsymbol{\rho}} (\boldsymbol{a}_z \times \boldsymbol{\kappa}_{rpq}) \tag{7}$$

For $z \geq d$

$$\boldsymbol{E}_3 = \sum_{r=1}^{2} \sum_{p=-\infty}^{\infty} \sum_{q=-\infty}^{\infty} b^{+}_{rpq} e^{-j\gamma^{o}_{pq} z} \cdot e^{-j\boldsymbol{k}_{pq}\cdot\boldsymbol{\rho}} \boldsymbol{\kappa}_{rpq} \tag{8}$$

$$\boldsymbol{H}_3 = \sum_{r=1}^{2} \sum_{p=-\infty}^{\infty} \sum_{q=-\infty}^{\infty} Y^{o}_{rpq} b^{+}_{rpq} e^{-j\gamma^{o}_{pq} z} \cdot e^{-j\boldsymbol{k}_{pq}\cdot\boldsymbol{\rho}} (\boldsymbol{a}_z \times \boldsymbol{\kappa}_{rpq}) \tag{9}$$

where $\boldsymbol{a}^{-}_{rpq}$, $b_{rpq}$, $\boldsymbol{a}_{rpq}$ and $b^{+}_{rpq}$ are unknown field amplitudes. The following boundary conditions should be satisfied for the scattered fields caused by the current density induced on the conducting elements of square spirals:

i) The tangential components of electric and magnetic fields are continuous at $z = d$,

ii) The tangential component of electric field is continuous at $z = 0$,

iii) The tangential magnetic field exhibits a jump discontinuity at $z = 0$ and is equal to surface current density which resides on the interface.

The boundary conditions are straightforward at $z = d$, resulting in,

$$a_{rpq} = R_{rpq} b_{rpq} \tag{10}$$

The continuity of electric field at $z = 0$ results in,

$$a^{-}_{rpq} = (1 + R_{rpq}) b_{rpq} \tag{11}$$

The third boundary condition on the tangential magnetic field at $z = 0$ is,

$$\boldsymbol{H}_2(x, y, 0) - \boldsymbol{H}_1(x, y, 0) = \boldsymbol{a}_z \times \boldsymbol{J}(x, y) \tag{12}$$

Substituting (5) and (7) into (12) and using (10) and (11), we find

$$\begin{aligned} &- \sum_{p=-\infty}^{\infty} \sum_{q=-\infty}^{\infty} \sum_{r=1}^{2} \left[ Y^{o}_{rpq} + Y_{rpq} \left( \frac{1 - R_{rpq}}{1 + R_{rpq}} \right) \right] a^{-}_{rpq} \cdot e^{-j\boldsymbol{k}_{pq} \cdot \boldsymbol{\rho}} \boldsymbol{a}_z \times \boldsymbol{\kappa}_{rpq} \\ &= \boldsymbol{a}_z \times \boldsymbol{J}(x, y) \end{aligned} \tag{13}$$

Taking the inner product on both sides of (13) $e^{j\boldsymbol{k}_{uv} \cdot \boldsymbol{\rho}} \boldsymbol{\kappa}_{ruv}$ (where $\{u, v\}$ are arbitrary integers), and integrating both sides of the resulting equation over one periodic cell (using the orthogonality relationship) we obtain the following expression for the coefficients $a^{-}_{rpq}$ in terms of the unknown induced currents.

$$a^{-}_{rpq} = -\frac{1}{A Y^{eq}_{rpq}} \int\limits_{\text{unitcell}} \boldsymbol{\kappa}_{rpq} \cdot \boldsymbol{J}(x', y') e^{j\boldsymbol{k}_{pq} \cdot \boldsymbol{\rho}'} dx' dy' \tag{14}$$

Hence the scattered tangential electric field for $z \leq 0$, can be written explicitly as,

$$\begin{aligned} \boldsymbol{E}_1 \;=\; &- \sum_{r=1}^{2} \sum_{p=-\infty}^{\infty} \sum_{q=-\infty}^{\infty} e^{j\gamma^{o}_{pq} z} \cdot e^{-j\boldsymbol{k}_{pq} \cdot \boldsymbol{\rho}} (Y^{eq}_{rpq})^{-1} \\ &\cdot \frac{1}{A} \int\limits_{\text{unitcell}} \boldsymbol{\kappa}_{rpq} \cdot \boldsymbol{J}(x', y') e^{j\boldsymbol{k}_{pq} \cdot \boldsymbol{\rho}'} dx' dy' \boldsymbol{\kappa}_{rpq} \end{aligned} \tag{15}$$

Since both the scattered and the incident field satisfy the dielectric boundary conditions, the final boundary condition is that the tangential electric field vanishes over the perfect conductor. Hence

$$\boldsymbol{E}_1(x, y, 0) + \boldsymbol{E}^{\text{inc}}_t(x, y, 0) = 0 \tag{16}$$

or substituting Equations (1) and (15) into (16), we find explicitly

$$\sum_{r=1}^{2}(1+R_{r00}^{\text{slab}})b_r^{\text{inc}}e^{-j\boldsymbol{k}_{00}\cdot\boldsymbol{\rho}}\boldsymbol{\kappa}_{r00} = \frac{1}{A}\sum_{r=1}^{2}\sum_{p=-\infty}^{\infty}\sum_{q=-\infty}^{\infty}e^{-j\boldsymbol{k}_{pq}\cdot\boldsymbol{\rho}}(Y_{rpq}^{eq})^{-1}\int_{\text{unitcell}}\boldsymbol{\kappa}_{rpq}\boldsymbol{J}(x,\,y)e^{j\boldsymbol{k}_{pq}\cdot\boldsymbol{\rho}'}dxdy\,\boldsymbol{\kappa}_{rpq} \tag{17}$$

where $b_1^{\text{inc}}=1,\quad b_2^{\text{inc}}=0$ for TM incidence,
$b_1^{\text{inc}}=0,\quad b_2^{\text{inc}}=1$ for TE incidence

Equation (17) is the Electric Field Integral Equation (EFIE) for the unknown current distribution. The most common method to solve EFIE is the MM. In the MM, the integral equation for the electromagnetic field is transformed into a simultaneous equation or matrix equation and the unknown quantities such as the surface current on conducting scatterers is evaluated by solving the simultaneous equation numerically. In Equation (17) the current density $\boldsymbol{J}(x,y)$ is approximated as follows:

$$\boldsymbol{J}(x,y)=\sum_{n=1}^{N}c_n\boldsymbol{f}_n(x,y) \tag{18}$$

where $c_n$'s are the unknown current coefficients to be determined. The functions $\boldsymbol{f}_n(x,y)$ are complete and orthogonal over a conducting element and N is finite for computability. Substituting (18) in (17) and integrating over a unit cell after multiplying both sides by $\boldsymbol{f}_m(x,y)$ yields the following system of equations.

$$\sum_{r=1}^{2}(1+R_{r00}^{\text{slab}})b_r^{\text{inc}}\boldsymbol{\kappa}_{r00}\cdot\boldsymbol{g}_{m00}^{*} = \frac{1}{A}\sum_{n=1}^{N}c_n\sum_{r=1}^{2}\sum_{p=-\infty}^{\infty}\sum_{q=-\infty}^{\infty}\frac{\boldsymbol{\kappa}_{rpq}\cdot\boldsymbol{g}_{mpq}^{*}\boldsymbol{\kappa}_{rpq}\cdot\boldsymbol{g}_{npq}}{Y_{rpq}^{eq}} \tag{19}$$

where $m = 1, 2, \ldots, N$ and the asterisk denotes the complex conjugate.

$$\boldsymbol{g}_{npq}=\iint\boldsymbol{f}_n e^{j\boldsymbol{k}_{pq}\cdot\boldsymbol{\rho}}dxdy \tag{20}$$

where

$$\begin{aligned}
\boldsymbol{k}_{pq} \cdot \boldsymbol{\rho} &= u_p x + v_{pq} y \\
u_p &= k \sin\theta \cos\phi + \frac{2\pi}{d_1} p \qquad v_{pq} = k \sin\theta \sin\phi - \frac{2\pi p}{d_1} \cot\beta + \frac{2\pi q}{d_2 \sin\beta} \\
\boldsymbol{\kappa}_{1pq} &= \frac{\boldsymbol{k}_{pq}}{|\boldsymbol{k}_{pq}|}, \quad \boldsymbol{\kappa}_{2pq} = \boldsymbol{a}_z \times \boldsymbol{\kappa}_{1pq}, \\
p, q &= -\infty, \ldots, -2, -1, 0, 1, 2, \ldots, \infty, \\
Y^{eq}_{rpq} &= Y^{o}_{rpq} + Y_{rpq} \left( \frac{1 - R_{rpq}}{1 + R_{rpq}} \right), \\
Y_{1pq} &= \frac{kY}{\gamma_{pq}}, \quad Y_{2pq} = \frac{\gamma_{pq} Y}{k}, \quad Y = \sqrt{\varepsilon/\mu},
\end{aligned}$$

$k$ is the propagation constant of the medium, $\varepsilon$ and $\mu$ are the permittivity and permeability of dielectric slab.

Once we select a suitable set of functions $\boldsymbol{f}_n$ the unknown coefficients $c_n$ can easily be obtained by solving (19). Since the solution domain is a contour, it can first be divided into small segments, denoted by $s_0, s_1, s_2, \ldots, s_N$ as illustrated in Figure 2 for one-turn square spiral FSS. The basis function $\boldsymbol{f}_n$, is used to approximately represent

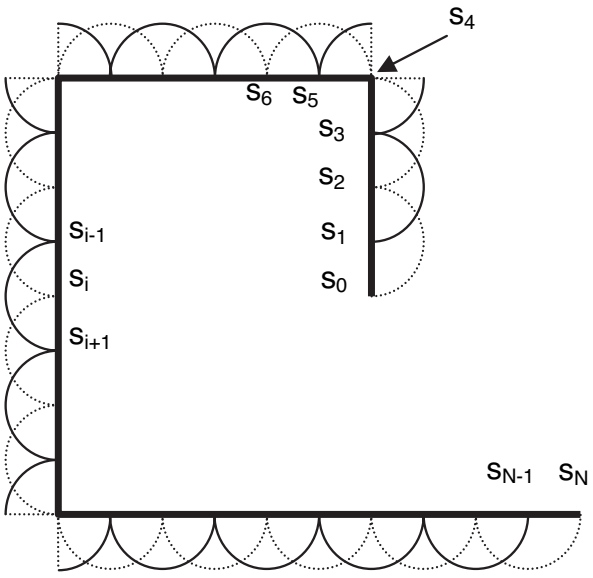


**Figure 2.** Piecewise sinusoidal expansion functions for one-turn square spiral FSS.

the surface current which is the overlapping functions of PWS. For the reason that the width of the square spiral ($w$) is too small compared to wavelength, the current density is assumed parallel to the axis of square spirals. The basis function in an arbitrary direction $\boldsymbol{a}_s$ is defined in parametric form as,

$$\boldsymbol{f}_n(s) = \boldsymbol{a}_s \begin{cases} \dfrac{\sin\beta(s - s_{n-1})}{\sin\beta(s_n - s_{n-1})} & s_{n-1} \le s < s_n \\ \dfrac{\sin\beta(s_{n+1} - s)}{\sin\beta(s_{n+1} - s_n)} & s_n \le s < s_{n+1} \end{cases} \tag{21}$$

where $\beta$ is the free space phase constant and $\boldsymbol{a}_s$ is the unit vector depending on the orientation of strips. The basis function in the first segment ($h_1$) is assumed to be in $\boldsymbol{a}_y$ direction and follows the contour of the FSS structure starting from the origin as illustrated in Figure 2 for one-turn square spiral.

The reflected and transmitted far fields contain only the propagating Floquet modes for which $\gamma_{pq}$ is real. By using a small array spacing, the higher order Floquet modes ($|p| > 0, |q| > 0$), which correspond to the grating lobes, are made evanescent. Thus the reflection and transmission coefficients are computed from the following expression for zero order propagating Floquet modes:

$$R = \sum_{r=1}^{2} \left\{ R_{r00}^{\text{slab}} b_r^{\text{inc}} - \frac{1}{AY_{r00}^{eq}} \sum_{n=1}^{N} c_n \boldsymbol{g}_{n00} \cdot \boldsymbol{\kappa}_{r00} \right\} \boldsymbol{\kappa}_{r00} \tag{22}$$

$$T = \sum_{r=1}^{2} \left\{ (1 + R_{r00}^{\text{slab}}) t_{r00} b_r^{\text{inc}} - \frac{t_{r00}}{AY_{r00}^{eq}} \sum_{n=1}^{N} c_n \boldsymbol{g}_{n00} \cdot \boldsymbol{\kappa}_{r00} \right\} \boldsymbol{\kappa}_{r00} \tag{23}$$

where $t_{rpq} = \frac{e^{j(\gamma_{pq}^o - \gamma_{pq})d} + R_{rpq} e^{j(\gamma_{pq}^o + \gamma_{pq})d}}{1 + R_{rpq}}$.

## 3. NUMERICAL RESULTS AND DISCUSSIONS

The numerical results of one- and two-turn square spiral FSSs backed by dielectric substrate are presented at normal incidence of TE and TM incident plane waves. The calculated reflection and transmission coefficients of one-turn square spiral FSS has been presented in Figures 3 and 4. The length of the first segment is $h_1 = 0.2\,\text{cm}$ and other lengths can be found from the relation $h_n = 2h_1(n-1)$ for $n = 2, 3, 4$. The width is chosen as one tenth of the first length ($w = 0.02\,\text{cm}$). The unit cell dimensions are $d_1 = d_2 = 1.55\,\text{cm}$. The number of Floquet modes used is $(2M+1)^2$, where $M = 12$. The

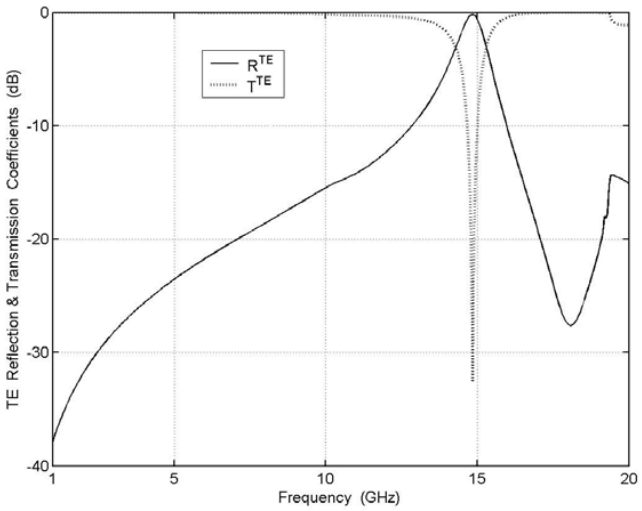


**Figure 3.** TE Reflection ($R^{TE}$) and transmission ($T^{TE}$) coefficients for one-turn square spiral FSS. ($d = 0.1\,\text{cm}$, $\varepsilon_r = 1.6$, $d_1 = d_2 = 1.55\,\text{cm}$, $w = 0.02\,\text{cm}$, $\theta = \phi = 0^\circ$, $h_1 = 0.2\,\text{cm}$, $h_n = 2(n-1)h_1$, $n = 2, 3, 4$.

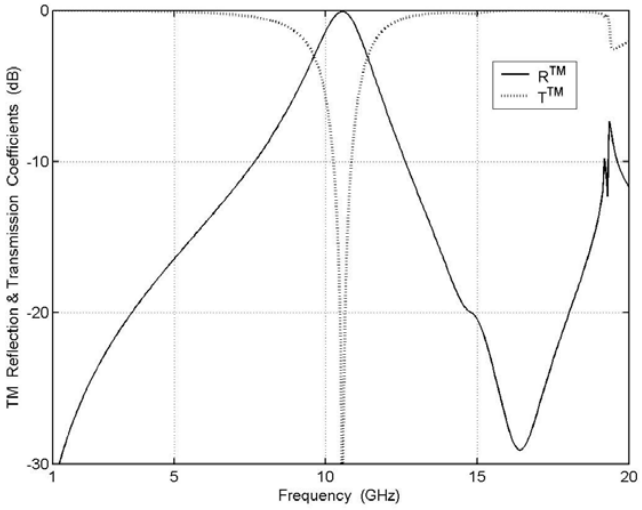


**Figure 4.** TM Reflection ($R^{TM}$) and transmission ($T^{TM}$) coefficients for one-turn square spiral FSS. ($d = 0.1\,\text{cm}$, $\varepsilon_r = 1.6$, $d_1 = d_2 = 1.55\,\text{cm}$, $w = 0.02\,\text{cm}$, $\theta = \phi = 0^\circ$, $h_1 = 0.2\,\text{cm}$, $h_n = 2(n-1)h_1$, $n = 2, 3, 4$.

only propagating mode is the zero order Floquet mode. The number of basis functions is 25 to determine the unknown current coefficients via the matrix inversion.

In Figure 3 we have a narrow band resonance for TE incident wave and the FSS structure is transparent up to about 12.5 GHz. The resonance happens at 14.8 GHz for TE incident wave. The bandwidth obtained for TM incidence is wider than that of TE case. The resonance frequency is at 10.6 GHz for TM wave incidence as shown in Figure 4. The propagating mode is the fundamental mode up to 19.2 GHz, and then higher order modes start to propagate for both type of polarization.

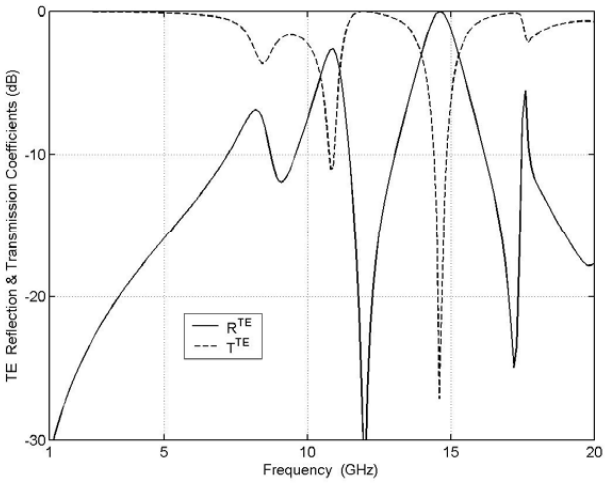


**Figure 5.** TE Reflection ($R^{TE}$) and transmission ($T^{TE}$) coefficients for two-turn square spiral FSS ($d = 0.1\,\text{cm}$, $\varepsilon_r = 1.6$, $d_1 = d_2 = 1.7\,\text{cm}$, $w = 0.01\,\text{cm}$, $\theta = \phi = 0^\circ$, $h_1 = 0.1\,\text{cm}$, $h_n = 2(n-1)h_1$, $n = 2, 3, \ldots, 8$).

The calculated reflection and transmission coefficients of two-turn square spiral FSS has been presented in Figures 5 and 6. The length of the first segment is $h_1 = 0.1\,\text{cm}$. The lengths of the other segments can be found from the relation $h_n = 2h_1(n-1)$, $n = 2, 3, \ldots, 8$. The overall length of the spiral is 5.7 cm. The width of the two-turn square spiral was chosen as $h_1/10$. The periodic cells are arranged in square lattice. The inter-element spacings $d_1$ and $d_2$ are 1.7 cm. The number of Floquet modes used is $(2M+1)^2$, where $M = 15$. This number is obtained by inclusion of more Floquet modes until there is little change in the results. The only propagating mode is the zero order

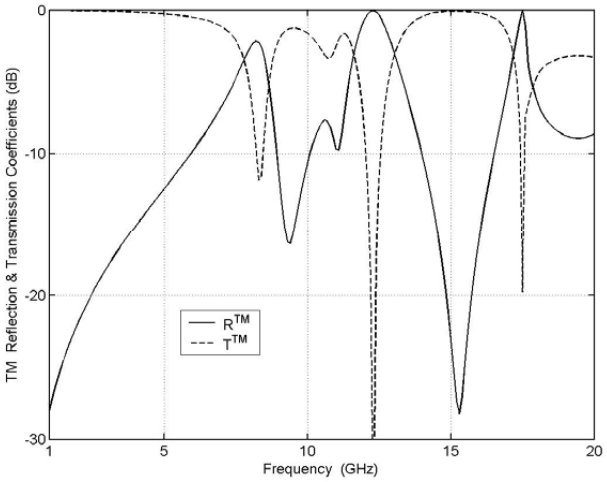


**Figure 6.** TM Reflection ($R^{TM}$) and transmission ($T^{TM}$) coefficients for two-turn square spiral FSS ($d = 0.1\,\text{cm}$, $\varepsilon_r = 1.6$, $d_1 = d_2 = 1.7\,\text{cm}$, $w = 0.01\,\text{cm}$, $\theta = \phi = 0°$, $h_1 = 0.1\,\text{cm}$, $h_n = 2(n-1)h_1$, $n = 2, 3, \ldots, 8$).

Floquet mode. The number of basis functions required to estimate the unknown current coefficients is 56.

In Figures 5 and 6, the reflection and transmission coefficients are plotted for dielectric backed two-turn square spiral FSS at normal incidence. The resonant frequencies for TE and TM wave incidences are different in the frequency range of 1–20 GHz, as shown in Figures 5 and 6. In Figure 5, there is a full transmission at the S-band frequency region (1–5 GHz) and the resonance frequency is at 14.6 GHz for TE incidence. The FSS comprised of periodic two-turn square spiral shaped conductors is used as a band stop filter in the microwave frequency regions of Ku-band. In Figure 6 there are two resonant frequencies for TM incident wave at 12.3 GHz and 17.5 GHz. The second resonant frequency is due to the higher order grating modes. The bandwidth of the second resonance is narrower than the first one.

## 4. CONCLUSIONS

The scattering of electromagnetic waves from a dielectric backed FSS of a new one- and two-turn square spiral shaped conductors are investigated by using the modal expansion method. The PWS basis functions are used to determine the unknown current coefficients. The

results of both FSSs show band stop filter characteristics at different frequencies while it is completely transparent at S-band frequency region. These structures are also transparent at some frequency regions. One resonance has been observed in the frequency range of 1–20 GHz for both types of FSS structures.

## REFERENCES

1. Munk, B. A., *Frequency Selective Surfaces: Theory and Design*, Wiley, New York, 2000.
2. Vardaxoglu, J. C., *Frequency Selective Surfaces: Analysis and Design*, Wiley, New York, 1997.
3. Nakano, H., *Helical and Spiral Antennas: A Numerical Approach*, Wiley, New York, 1987.
4. Delihacıoğlu, K., S. Uçkun, and T. Ege, "Scattering characteristics of FSS comprised of L-shaped and one-turn helix shaped conductors for TE and TM excitation," *Electrical Engineering*, Vol. 89, No. 3, 177–181, 2007.
5. Delihacıoğlu, K., S. Uçkun, and T. Ege, "Frequency selective surfaces comprised of periodic arrays of two-turn square spiral shaped conductors," *Int. J. Electron. Commun. (AEÜ)*, Vol. 61, No. 3, 182–185, 2007.
6. Harrington, R. F., *Field Computation by Moment Methods*, MacMillan, New York, 1968.
7. Amitay, N., V. Galindo, and C. P. Wu, *Theory and Analysis of Phased Array Antennas*, Wiley-Intersec., New York, 1972.
8. Montgomery, J. P., "Scattering by an infinite periodic array of thin conductors on a dielectric sheet," *IEEE Trans. Antennas Propagat.*, Vol. 23, 70–75, 1975.